CROSS-FOLDING BY DIFFERENTIAL INTERFERENCE

E. S. O'DRISCOLL. B.Sc.

Dept. of Economic Geology,
University of Adelaide,
Adelaide, South Australia.

CONTENTS

PREFACE

The concept of cross-folding is as well established in the science of geology as the concept of shearing. Almost any technical report on the geology of an ore deposit, particularly if the ore is of Palaeozoic or Pre-Cambrian age, will refer to the influences of shearing and cross-folding in the history of ore deposition. Of particular interest are the types of folds known as "similar folds" (or "shear folds"), so commonly found in ancient geologic structures, and in which the qualities of both folding and shearing are inter-dependent.

The following thesis is an exposition of some of the qualities of structural morphology that are inherent in the combination of shearing and cross-folding where the shearing is specified as simple shear involving differential planar movement by laminar flow imposed on specified surfaces which are thereby deformed into folded shapes. The exposition is achieved by means of laminar models in which the required specifications are inscribed.

STATEMENT

This Thesis contains no material which has been accepted for the award of any other degree or diploma in any University, and, to the best of my knowledge and belief, it contains no material previously published or written by another person, except where due reference is made in the text of the thesis.

Signed:

E.S. O'DRISCOLL

CROSS-FOLDING BY DIFFERENTIAL INTERFERENCE

ABSTRACT

Experimental studies of the shapes of surfaces resulting from the interference of two intersecting systems of similar folds have been carried out by means of three-dimensional models consisting essentially of vertical laminae parallel to the axial planes of the intersecting fold systems. The edges of these laminae form a continuous surface on which the cyclic anticline-syncline profiles of the component folds are produced by differential vertical shear movement parallel to the respective axial planes. The mutual interference of the component profiles results in a continuous interference surface consisting of alternating domes, basins and cols which represent the spatial relationships between centres of maximum and minimum interference. Any plane truncating such a surface exposes shapes variously transitional from linear to circular or elliptic form, and possessing both axial and quadrantal symmetry. It can be shown that sigmoid flexures, echelon alignments in a horizontal plane, and non-vertical fold axial planes can result exclusively from vertical shear movements and their mutual interference. Where such interference profiles are imposed through vertical axes on a succession of mutually inclined surfaces, the resulting successive structural closures on these surfaces do not remain centred on a vertical axis but undergo various lateral migration according to the individual dips of the surfaces. A superimposed uniform differential movement may even cause the disappearance of particular closures.

INTRODUCTION

This paper describes some experiments in laminar deformation which the writer carried out as a project during the year 1961. The experiments were developed in the form of three-dimensional models to allow the study of the topological transformations under the influence of simple shear movements, and in the mathematical analysis of resultant shapes, considere independently of conventional stress-strain mechanics (which, however, is quantitatively inherent in models but simply not to scale).

The writer had worked for many years on Precambrian strata where defined similar folding was much in evidence, and where cross-folding had produced biaxial systems in which it was difficult to assign a priority in time to either of the component folds. Indeed, simultaneous folding on both axes could have been readily acceptable, with the reservation that the criteria of such simultaneity might well be obscured by the complexity of Precambrian deformation. Later observations in less deformed Palaeozoic and younger rocks, in which sedimentary patterns appeared to indicate synchronous cross-folding, led the writer to suppose that such cross-folding owe its topological character principally to differential movement in the direction of the vector common to both fold systems, viz. parallel to the inter-section of their respective axial planes, and that the dominant quality of such folding was

closely in accordance with the concept of defined similar folds produced more by vertical than by horizontal differential forces. These considerations led the writer to wonder what were the invariants and the maximum possible topological effect of similar folds deformed by uncomplicated simple shear differential, and to investigate the patterns produced on surfaces by the mutual interference of two intersection systems of such folds. This was obviously a mechanism of defined similar folding, and therefore, in essence, susceptible of geometric demonstration by laminar models deformed by planar adjustment. To allow this, a series of laminar models was made to simulate the deformation of a given surface or surfaces both by single folding and by cross folding imposed exclusively through vertical shear movements. The technique of laminar model demonstration offers a particular advantage. Whereas conventional deformation studies are usually carried out with postulated stresses, laminar model deformation jumps a step farther by postulating the <u>strain</u>. This circumvents the need to specify physical quantities such as elasticity, viscosity, time etc., on which the strain depends.

The mechanism of laminar model deformation is consistent with the conception of "shear-folding". In practice the writer prefers to avoid the term "shear" where it necessarily connotes visible planar qualities, and to regard the differential movement as a continuous function with or

without visible shearing.

PREVIOUS WORK

The writer received his initial inspiration from the admirable exposition by Carey (1954) of the rheid concept in geotectonics. It subsequently occurred to the writer that many rheid shape transformations could be adequately demonstrated only by the use of laminar flow models where the mechanism of deformation and its movement were clearly and physically represented. The various laminated models constructed have been demonstrated to a number of informed authorities both from Australia and overseas, and through them the writer believes that the demonstrations described in the following paper constitute a new approach leading to new conclusions affecting fundamentals of deformation.

LAMINAR MODELS

The basis of the models is a pack of plane card laminae (see Fig. 1) which represent the axial planes of a system of similar folds. When such a pack is supported vertically and the bottom edges pressed into a "fold mould", T, the profile of the mould is transmitted to the top of the pack by virtue of the differential shear movement between the laminae, and the resulting shape of the upper surface of the pack is considered as the first set of folds of a subsequent

cross-fold combination. Thus in Fig. 1, the fold axes of this first set of folds lie horizontally in the direction A-B which is also the strike of the vertical axial planes. The problem is how to cross-fold the shape of this surface by a second similar fold-mechanism.

There are technical difficulties in devising a pack of cards in which the card planes run in both axial directions at once (requiring linear elements instead of planar elements) and therefore the first set of folds is "transferred" from the first pack to a second pack with laminae striking in the second (or cross-fold) direction. This is achieved by cutting the first set of folds transversely into the upper surface of the second card pack (see Fig. 2) with the precise shape it has assumed when formed by differential shear movement on transverse vertical planes of the first fold system.

Fig. 3 shows how this pack is then moulded into a longitudinal fold template T, which, by differential vertical movement of the cards, imposes the second set of intersecting folds upon the first set. In Fig. 3 the first set of folds has its axial trend in the direction A-B, and the second set, moulded by the template T, its axial trend along C-D. The resulting interference surface is produced at the top of the pack. It is important to emphasise that because the sequence of fold imposition is arbitrary, and because the first folds

cut into the pack are as if produced by differential movement on a conjugate transverse card direction A-B, the interference surface is such as would be produced by simultaneous differential movement on two coexisting intersecting card surfaces, or "axial" planes, in the pack. These two plane systems in Fig. 3 are vertical, obliquely intersecting, with differential movement vertically in the direction of their intersection. The two component profiles are chosen as simple sine curves, and the interference surface is a sinusoidal surface showing a checkerboard pattern of "domes", cols and "basins" arranged en echelon, and representing the spatial relationships of centres of maximum and minimum interference between the two component fold systems.

FOLD INTERFERENCE PATTERNS

Figures 4-9 show the interference patterns produced by variation of wavelength in the first set of intersecting folds. In Fig. 4 the card models shows the first folds cut in the direction A-B, with the wavelength (and amplitude)small near the centre, and larger at either end. Fig. 5 shows this system with the second set of vertical folds, (C-D) imposed on it by the template T, and the resulting echelon pattern formed without any horizontal shear component. It can be seen that the echelon may be described as left-hand for the small folds along the C-D axis, or right-hand for the larger folds on the

ridge through D, parallel to A-B.

Fig. 6 shows this interference surface with small quantities of mercury poured into the "basins" in order to show the axial and echelon directions which appear to be progressively "rotated" with the successive variations in wavelength. Owing to its high surface tension the mercury does not wet the cards nor seep between them by capillarity.

Fig. 7 shows the same surface with the depth of mercury increased to show the attendant change in basin boundaries from elliptical to rhomboid form. The development of sigmoid flexures can be seen at B, and is due to differential vertical movement and not horizontal movement.

Fig. 8 shows the interference surface of a rectangular equidimensional cross-fold system, with mercury at different depths in the basins to show the transition from circular boundaries (A) in the deeper parts to square boundaries (B) near the col levels.

In Fig. 9 the interference surface is the result of a continued progressive decrease in the wavelength of the first fold system (axis A-B), with a consequent progressive rotation of the axes of the individual structures. Thus, the axes of successive basins, taken from corner B across to corner C, form an arcuate link, convex to the right, joining the two basic fold trends. The echelon pattern is left-hand along trend A-B , and right-hand along the trend C-D. It is of interest

to note that in the succession of domes X, Y and Z, X and Z show opposite sigmoid flextures about the neutral form in Y.

Fig. 10 is a composite tracing of Figs. 6 and 7 to show variations in basin boundary shapes with depth. The black centres represent the shallow mercury fillings of Fig.6 and the surrounding outlines the deeper mercury fillings of Fig. 7. It will thus be seen that the direction of the long axis of the basin varies with depth. The progressive "rotation" of basin axes, marked e-a to e-f, may be clearly seen trending in left-hand echelon parallel to C-D. e-f is also part of a right-hand echelon system e-f, e-g, e-h, parallel to A-B. The coexistence of left-hand and right-hand echelon, (both produced exclusively by vertical differential movements), shows that such definitions can be arbitrary, or a matter of scale and relative prominence.

Let us consider the basic topography of a simple symmetrical interference surface, as shown in the relief plan in Fig. 11, formed by the intersection of vertical differential movements in the axial planes of the two fold systems. Here the first fold system has its axes oriented east-west (parallel to the F_1S_1 direction) and is intersected at right angles by the north-south axes of the second fold system (parallel to the F_2S_2 direction). The profiles of the fold systems have been given equal amplitudes but unequal wavelengths, and are simple sine curves of the type $y = \sin x$ and $y = \sin z$,

producing a sinusoidal interference surface of the type y = (sin x + sin z). This results in a pattern of domes (marked H for "high") and basins (marked L for "low) with connecting saddles or cols (marked C). The H and L points mark the centres of maximum mutual augmentation of the positive and negative maxima of the two fold systems, whereas the C points mark the centres of mutual symmetric opposition of these qualities.

The sequence of structures in the two basic fold directions (N-S and E-W) is in each case a succession of dome-col-dome (H-C-H), or basin-col-basin (L-C-L), whereas the sequence in the two quadrantal directions (NE-SW and NW-SE) is in each case a succession of dome-basin-dome (H-L-H), alternating with lines of col-right homocline-col-left homocline-col. It is important to note that the pattern and shape of the interference surface is independent of whether the two fold systems are imposed simultaneously or in arbitrary sequence, provided that the continuity of the surface is maintained (i.e. neither truncated nor faulted). In Fig. 11 two contour levels of a central basin have been accentuated in order to show the transition from elliptical form at the centre to rhombic form at the edges. The basin is thus seen to possess a quadrantal variation in symmetry and to be bounded by four linear hinges, joining the four associated col points, along which the surface dip varies from zero at the

cols to a maximum alternating to right and left midway between them. It should also be noted that because the interference pattern is repeated for all parallel strata that might be inscribed through the model, the two contours that have been accentuated (and all others as well) also represent the traces of successive strata as they would be exposed on a horizontal plane of truncation.

The system of lines F_1-S_1 and F_2-S_2 are drawn respectively midway between the crests and troughs of the two intersecting fold systems. These lines thus represent the loci of maximum shear respectively for each system, and their intersections mark the centres of maximum total shear intensity at the interference surface. The shear gradient around these centres of maximum shear is determined by the differential coefficient of the interference surface which is a direct function of the total shear intensity. If the shear gradient is contoured in the given model, the contours around the loci of maximum shear will show elliptical (to rhombic) boundaries with vertical linear extensions in depth. These loci lie on the conjugate linear trends - the C-C hinges - which are lines of rhythmic reversals of vertical shear movement.

In the topological transformations demonstrated by the foregoing models, the echelon alignments of shapes and directions may be regarded as interference phenomena resulting from the axial migration that is inherent in differential shear

movement. Such axial migration is due to the mutual interference of the gradients of the two intersecting fold profiles. Two such profiles are shown separately in Fig. 12 (i) aligned in the required position prior to their mutual interaction. The large anticline A is equivalent to the first fold profile cut into the cards of a model; the series of smaller folds is equivalent to the second profile regarded as a template from which the anticlinal axes a1, a2, etc. are transmitted through to the upper surface of A by vertical laminar movement. Fig. 12 (ii) shows the interference profile resulting from the interaction of the two systems when the one is superimposed upon the other by this process. The crests a1, a3, a5 are transmitted to points on the A profile where the gradient of the latter is zero, and therefore there is no lateral migration of the axial lines. However, the crests a2 and a4 are transmitted to points on the A profile where the gradient of the latter is not zero, and the resulting differential interference causes the anticlinal axes to be offset up-slope to positions a'2 and a'4. Similarly the synclinal axes are offset in the opposite direction, and it is this differential migrational phenomenon that produces echelon disposition in interference folding at the intersection of axes.

Figs. 13 and 14 show how both right and reverse sigmoid flexures can be produced in the horizontal plane by the differential interference of vertical movements where the

amplitude only is changed.

Fig. 13 shows a contour relief plan of the differential interference dome resulting from the interaction of anticline A-A, of amplitude approximately 10 units, with the anticline B-B of exactly equal wavelength but amplitude of 5 units. It can be seen that the mutual coalescence of the intersecting axial crests causes the interference dome to be aligned into the acute angle of the axial intersection and that anticlinal continuity is maintained along the A-A axis by means of a right sigmoid connection. This is due to the amplitude and rate of crestal curvature of the A-A anticline being greater than that of B-B.

In Fig. 14 the anticline B-B is replaced by another C-C, which has an amplitude twice that of A-A. In this case, crestal continuity is maintained in the C-C direction by means of a reverse sigmoid connection. In each case there is no horizontal movement involved, and the only difference in the formation of opposite sigmoid flexures is in the relative rate of crestal curvature of the components folds, here expressed as difference in amplitude.

Fig. 15 is virtually a combination of the principles of Fig. 13 and 14 to show the co-existence of opposing sigmoidal domes produced synchronously by vertical movements only. As before, the two component systems are different vertical shear-fold profiles of the same wave-length with their

axial trends approximately 45 degrees apart. Their amplitudes have been chosen to differ so that the single anticlinal ridge A-A', of intermediate amplitude, (see sectional profile at lower left of Fig. 15) is superposed in a NNE direction on the second system of folds trending NNW and consisting of two anticlines, B-B ' and D-D', of smaller and greater amplitudes respectively, flanking a medial syncline, C-C' (see sectional profile at lower right of Fig. 15.

All the fold-producing movements in Fig. 15 are specified as being vertical, and thus the superposition of the one vertical anticlinal fold (A-A') on the pre-existing relief of B-B' and D-D' has formed contemporaneous sigmoidal domes seemingly in opposing senses. In Fig. 15 a contour interval at the saddle level of each dome has been stippled to illustrate these coexisting opposite sigmoidal shapes. A conventional explanation of such shapes would invoke transcurrent rotational movement. Indeed, the coexistence of the opposing sigmoidal domes might invite the supposition of separate independent and opposite horizontal rotational movements. However, in this case, the shapes result from vertical movements only. It will be seen that the trends (elongations) of the crestal closures (top contours) of the two domes do not coincide with either of the basic axial directions. This emphasizes the need for care in determining fold axial directions from the shapes of dome tops, since the crestal shapes are often the only part of such

structures that are well known.

In Fig. 16 the interference surface produced by two relatively large anticlines (A1, A1 ... of No. 1 profile) which are intersected obliquely by four smaller anticlines (A2, A2 ... of No. 2 profile) is an example of the interplay of both right and reverse sigmoids, with right-hand and left-hand echelons. Since the A2 folds have the greater rate of crestal curvature, they maintain their crestal continuity through the complex, and establish the sigmoid links through the col areas. The wavelength of the folds appears to be the dominant factor in the echelon orientation of the mean axes of the sigmoid flexures. It should be noted in Fig. 16 that the orientation of the S1-S2 basins is different from the orientation of the A1-A2 domes. The echelon disposition is left-hand along the A1 axes and right-hand along the A2 axes.

It is interesting to observe the disposition of centres of maximum shear intensity in the case of non-rectangular intersection of variable folds exemplified in Fig. 16. For perspective clarity, the shear intensity pattern of Fig. 16 has been replotted in Fig. 17 as a generalised version. Only the essential framework has been reproduced showing the elliptical areas of maximum shear in their spatial relationship to the "cross-folded" domes and basins lying along the principal anticlinal and synclinal trends. Here the quadrantal symmetry previously seen in the symmetrical rectangular system

of Fig. 11 is biased by the oblique axial intersection which introduces the echelon quality. The axes of the elliptical loci of maximum shear do not coincide with those of either the domes or the basins, and the individual shear directions within the ellipses are themselves oriented in a different direction. These individual shear trends are shown within the elliptical shear zones in Fig. 17 as lines striking approximately NNE.

TRACES OF RANDOM SECTIONS

In order to examine the patterns revealed by a succession of interference surfaces when truncated by a plane, a type of card model has been devised in which each card not only has the profile of the "first" fold system cut into its upper edge, but also has printed upon it a succession of similar-fold profiles representing successive surfaces of the one fold system in depth. The pack of such cards has then been cross-folded in the manner already described, thus producing the interference surface of domes and basins not only on the top of the pack, but also repeated internally in the pack for each successive surface. Selected plane sections have then been cut through the card pack to expose the traces of the interference surfaces.

Fig. 18 shows a specimen of the type of card used in the models to be described. As used, the cards are unmarked except for the succession of similar fold profiles printed

upon them. For the purpose of this description, notations have been added to the specimen card in Fig. 18. The similar fold profiles represent the "first" fold system, with vertical axial planes parallel to A-A and S-S, which mark the anticlines and synclines of the accentuated stratum on the card. The lines P-P mark the loci of maximum shear on the limbs of the folds. In the figure they have equidistant spacing. The line M-M represents the slopes of a larger structure on which the smaller fold profile has been imposed. It may be regarded as a "regional" gradient or differential. For reasons already described the axes A-A and S-S are therefore not equidistantly spaced. Although terminology in these matters is not confirmed the writer has rather loosely employed the prefixes "micro-" and "mega-" to denote scales relative to the basic elements. In this way the line M-M has been regarded as the slope of a "mega-structure" on which the basic profile is imposed. The profiles in Fig. 18 have been described as anticlines on a "meganticline" (or domes on a "mega-dome") and the line M-M has accordingly been described as defining the "mega-slope".

Fig. 19 shows a printed card model in which the continuous interference surface of domes and basins is seen intact in the upper foreground. On the vertical plane X of the cards may be seen the printed profile of the first-fold system. On the vertical plane Y is the profile representing

the second-fold system. Where the cut edge of a card intersects a printed fold trace, a dark spot shows on the edge, and when a stack of cards is guillotined or ground down, these spots link up to form the trace of the interference fold surface as seen on that plane of section.

The upper rear surface of the pack has been planed to expose the traces of the interference surfaces which emerge in the form of domes (H) and basins (L). One stratum has been accentuated for illustrative purposes. The "mega-slope" of the pack can be conceived as a plane dipping toward the observer and tangential to the domes of the intact interference surface. Its strike in this particular model therefore approximately bisects the angle between the two basic fold axes.

The bottom of the pack has been planed horizontally to reveal the essential geometry of the differential interference fold traces on a plane mutually perpendicular to the axial planes of the two fold systems. A photograph of the planed bottom of the pack is shown in Fig. 20 which has not been retouched except to pick out one formation with stipple. The traces shown are simply the cut ends of the printed folds on the faces of the cards. The two axial shear directions are shown striking N-S and E-W, and the stippled stratum trending NE represents the strike of the "mega-slope". The dip of the mega-slope may also be inferred from the geometry

of the continuous stratum which separates basins on the down-slope side (NW) from domes on the up-slope side (S.E.).

Fig. 21 shows the planed bottom of a similar model which differs in having the "mega-slope" striking N-S parallel to one of the basic shear directions, and dipping to the west. From these figures it may be seen that the "mega-slope" attitude can determine the predominance of quadrantal or axial strike-trends where the axial planes are perpendicular to the exposed surface.

Fig. 22 shows configurative variations exposed by curved surfaces cut on a pack. These produce an effect equivalent to inclining the axial planes of the interfering folds to the surface of exposure.

IMPOSITION OF SIMILAR FOLDS ON INCLINED SURFACES

Figs. 23-26 show the effect of imposing a regular shear fold profile on a succession of surfaces (or strata) that are not parallel. Fig. 23 shows a vertical card-model surface inscribed with the traces of a succession of variously inclined surfaces, and ready to be moulded into the fold template T for which the anticlinal and synclinal axes are marked, respectively, A1, A2 and S. Two different strata, X and Y, have been accentuated for reference. Fig. 24 shows the model after the imposition of the template profile by differential movement on the vertical axial planes. The original equally spaced

vertical axes A1, S and A2 are now seen to be discontinuous, curved and variously offset in the different groups of strata, the anticlines moving up-dip and the synclines moving down-dip, with respect to the strata. Anticlines in the X stratum do not coincide vertically with those in the Y stratum although both have been subject to the same vertical differential movements.

Figs. 25 and 26 show further horizontal migrations caused by applying both clockwise (Fig. 25) and anticlockwise (Fig. 26) "regional" shears to the same model depicted in Figs. 23-24. The effects on axial spacing and the disappearance of some structural closures are particularly noteworthy. The original boundaries of two such structural closures shown in the Y stratum in Fig. 24 are seen in Fig. 25 to have become off-set and tilted by deformation to an angle which virtually deprives them of their original closures. As before, rotation has caused axial planes, drawn conventionally in relation to the respective individual folds, to be inclined to the vertical.

The models in Figs. 23-26 are two-dimensional illustrations of axial migration on particular inclined sectional profiles. The three-dimensional effect of such migration can be seen in Fig. 27 where the wavy trace AaBbC represents the edge of a cross-folded horizontal surface extending through the card pack, and the trace Dd'dEe'F

represents the edge of an inclined surface forming the upper surface of the pack and cross-folded by the same movements. Both surfaces, originally plane, have been cross-folded by the same horizontal similar folds with axial directions respectively BA and BC and intersecting at right angles, and with vertical differential movement on vertical axial planes. The inclined surface is shown striking obliquely to both fold axes.

As before, the crests, a and b, of the anticlines in the horizontal folded surface, ABC, do not coincide vertically with the corresponding crests, d' and e', of the anticlines in the inclined folded surface DEF, but are offset laterally by distances proportional to dd' and ee'. It can be seen that the axial planes of the component folds in stratum ABC, passing respectively through ad and be, intersect along a vertical line through f, which marks the plan position of the interference dome on the undersurface ABC (in depth). On the other hand, the vertical axial planes of the corresponding folds in the DEF surface passing respectively through d' and e'. intersect along a vertical line passing through f', which marks the plan position of the corresponding interference dome on the upper surface DEF. Thus in composite plan the crest of the dome f' on the upper surface DEF, is displaced laterally from the crest of the corresponding dome on the undersurface ABC, in depth vertically below f. This lateral displacement

is effected entirely by vertical movements in the interfering fold systems. The direction of domal migration from f to f' depends on the attitude of the inclined upper surface DEF with respect to the horizontal undersurface ABC. Where the strike of surface DEF is parallel to BC, EF becomes horizontal and f' moves in the direction of BC.

CONCLUSIONS

The foregoing experiments illustrate some of the effects of similar fold mechanisms involving simple shear. Analogies drawn between experimental observations and field occurrences are, of course, subject to the accepted qualifications of inductive reasoning and must make due allowance for the factors that cannot be represented in model experiments. The writer is convinced, however, that a proper understanding of the limitations of similar-fold mechanisms is impossible without prior understanding of the various topological transformations that such mechanisms can effect in their simple essential form.

It will be seen that care must be exercised in accepting conventional evidence for horizontal or rotational movements if such evidence is based solely on structural shape patterns. It is considered significant that the basic patterns of echelon alignments and sigmoid flexures can be produced in the horizontal plane by the interference of two fold systems

formed exclusively by vertical movements. Echelon alignments and sigmoidal structures are therefore not necessarily evidence of transcurrent rotational movements; nor is the coexistence of both right-hand and left-hand echelon sigmoidal domes necessarily evidence for two opposing systems of horizontal movement.

Conspicuous lineaments such as straight basin boundaries and straight hinge lines may have no connection with faulting. Cross-folding by vertical movements alone can produce such linear qualities which emerge as natural interference phenomena.

It is considered significant that the mechanism of regular and continuous interference may, by vertical movements alone, cause fold axes to undergo horizontal dislocation and deflection where they transect surfaces of unconformity. Similarly the curving of fold axes in depth is not necessarily evidence of lateral compression or bedding plane glide but merely a response to vertical differential movement. The possibility of such movement having taken place in gently folded structures without visible shearing may be consistent with the type of uniform creep that can be demonstrated experimentally in the deformation of plastic material by laminar flow, where the material behaves geometrically as a "shear-fold", but exhibits no visible shearing.

ACKNOWLEDGEMENTS

The author desires to record grateful acknowledgement to the Director of Mines, South Australia, for permission to submit the work for a thesis; to Professor E. A. Rudd, University of Adelaide, for valuable guidance during the preparation; to Professor Carey, University of Tasmania for criticising the manuscript; and to Mr. F. Koltai, Visual Aids Branch, Educational Department for photography of models.

REFERENCES

CAREY, S.W., (1954) "The Rheid Concept in Geotectonics", Jour. Geol. Soc. Aust. Vol. I, p.67-117

O'DRISCOLL, E.S., (1962) "Fold Interference Patterns in Model Experiments". Nature. Vol. 193., No. 4811, pp. 115-117.

FIGURE 1

The pack of plane laminar cards which is the basis of the experimental models. The fold mould, T, transmits its shape to the top of the pack to produce the first fold system with its axial direction A-B .

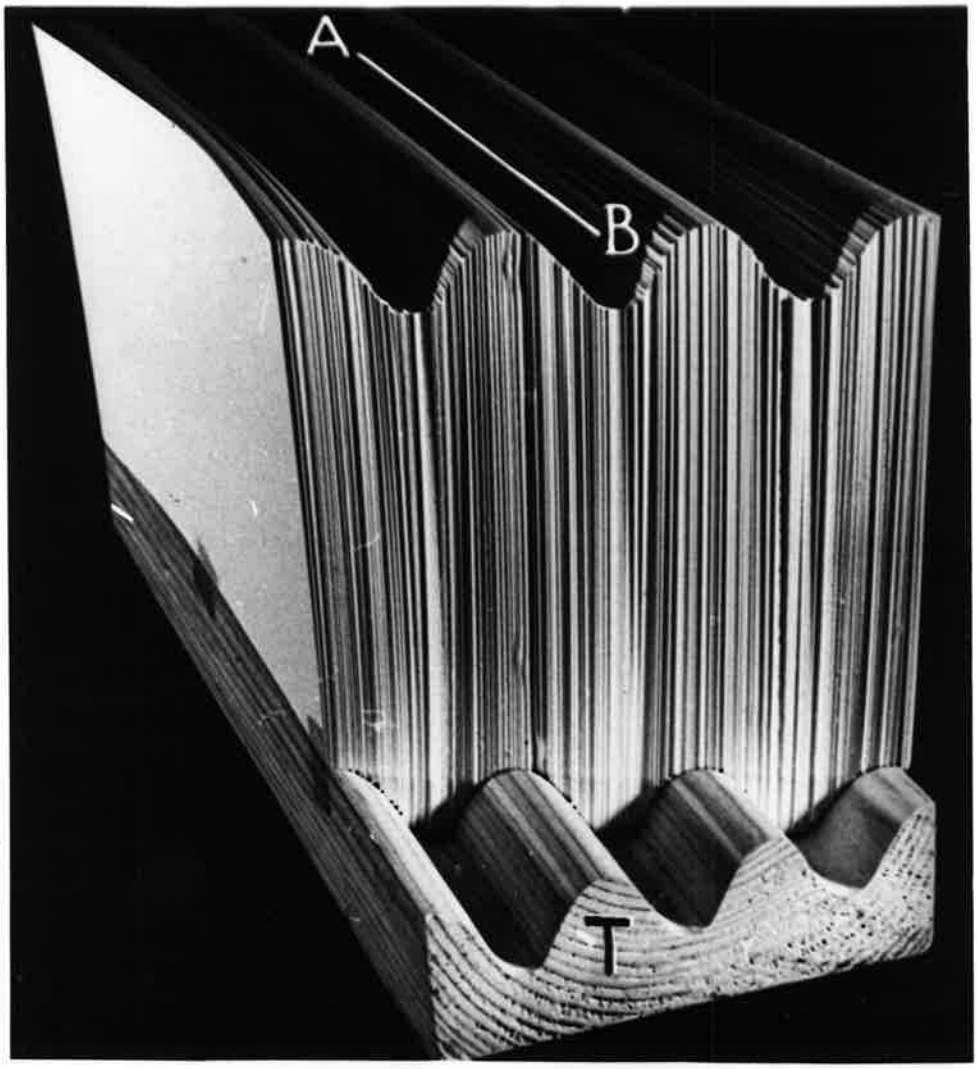

Fig. 1

FIGURE 2

The profile of the first similar-fold system reproduced in a transverse direction on the upper surface of the card pack. The fold System A-B is that of the fold mould T (as seen in Fig. 1).

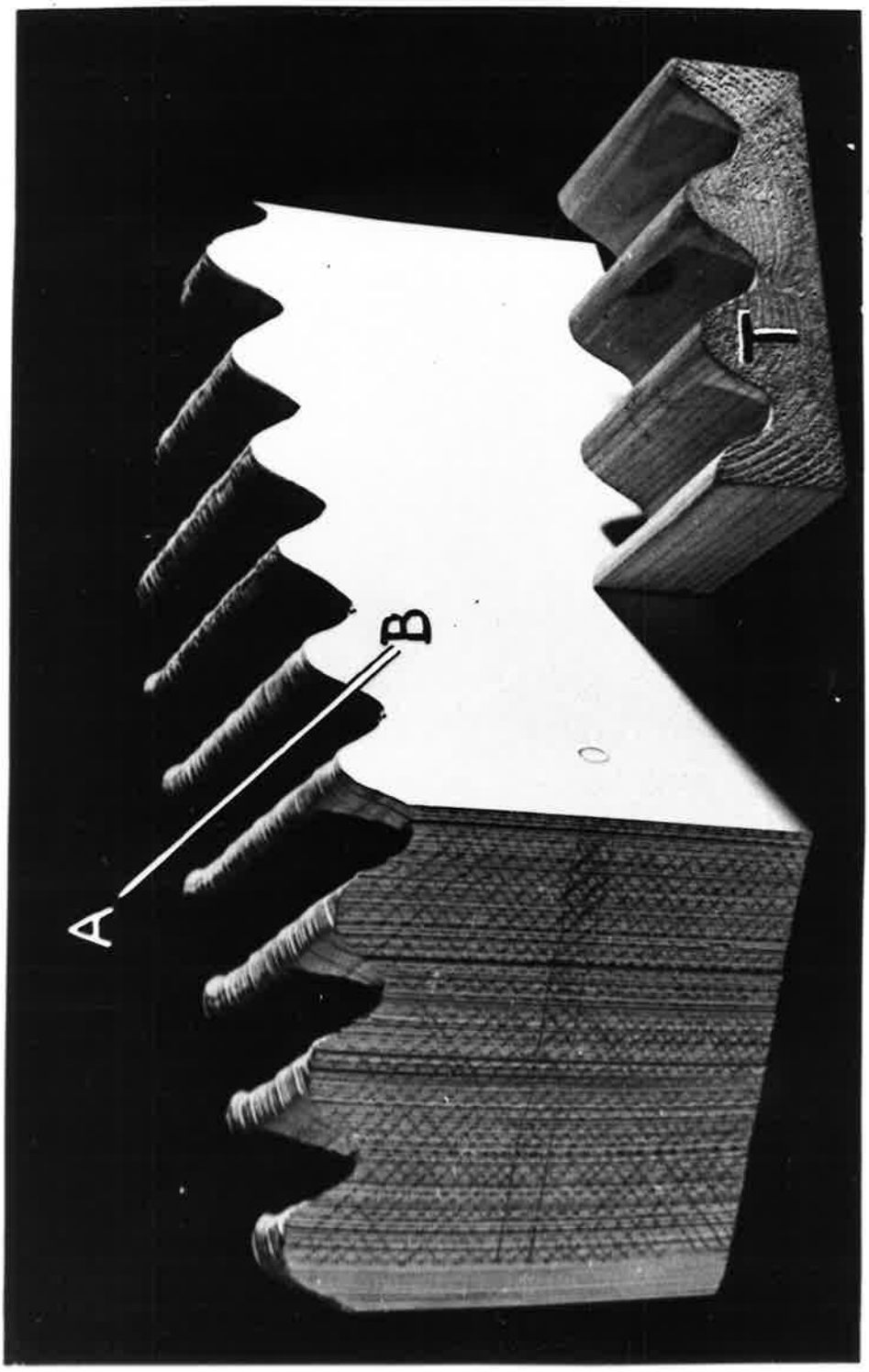

Fig. 2

FIGURE 3

The pack previously shown in Fig. 2 with the transverse first-fold system, A-B, is moulded on the template, T, which now transmits a longitudinal equidimensional second fold system, C-D, to the top of the pack to form an interference fold surface of domes and basins aligned en echelon.

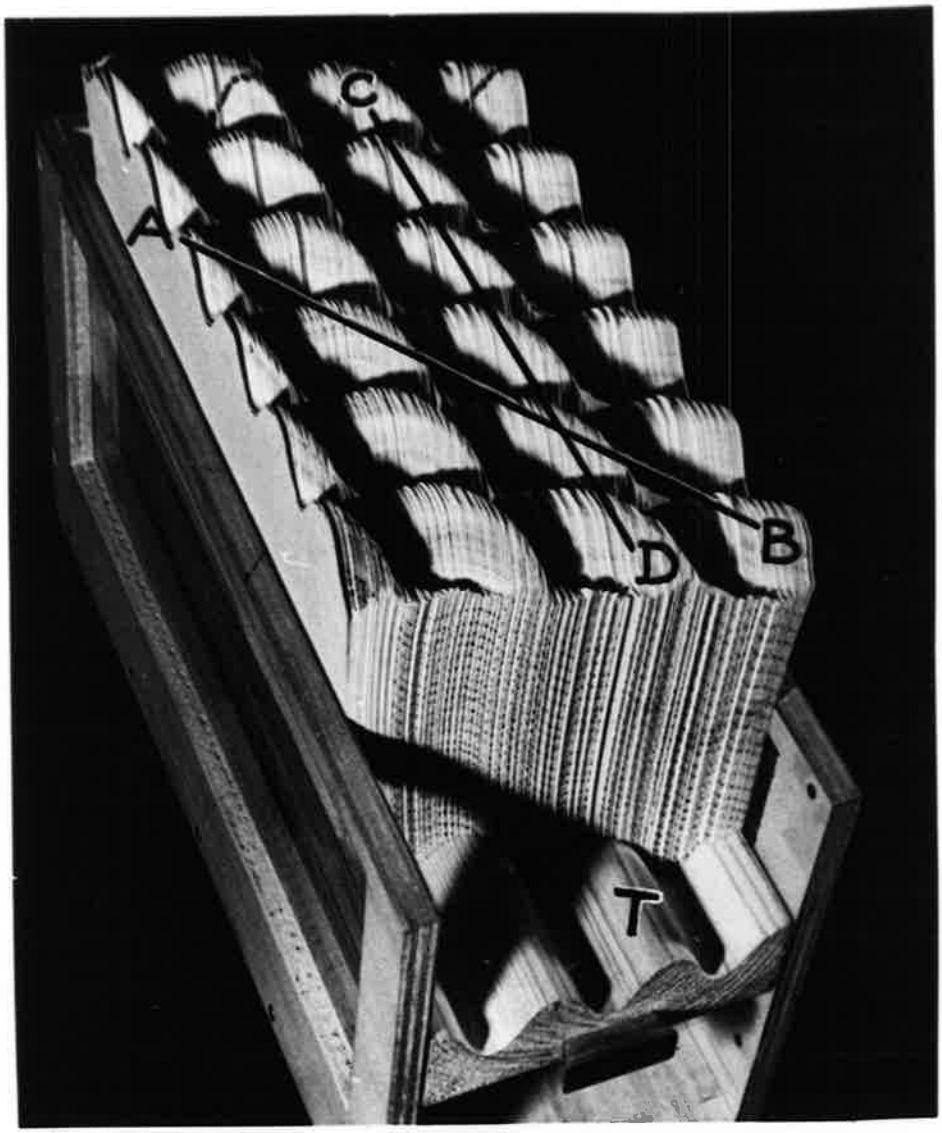

Fig. 3

FIGURE 4.

A card pack incorporating a first-fold system, A-B, in which the wavelength and amplitude are varied. Axial planes are vertical.

Fig. 4

FIGURE 5

The same card pack of Fig. 4 now has the second vertical fold system, C-D, transmitted by the template T to the top of the pack to produce a vertical differential interference fold surface with various sigmoidal en echelon alignments.

Fig. 5

FIGURE 6

The same surface as in Fig. 5 with small quantities of mercury poured in the "basins" to emphasize the resultant en echelon axial directions.

Fig. 6

FIGURE 7

The same surface as in Fig. 6 with more mercury added to show the rotation in azimuth of "basin" axial directions with depth, and the change from elliptical to sigmoidal outlines near col level.

Fig. 7

FIGURE 8

Orthogonal equidimensional system of differential interference folds with mercury added to show the variation of structural outlines from circular to square form as at "A" and "B" respectively.

Fig. 8

FIGURE 9

A fold surface in which the wavelengths and amplitudes of system A-B are continuously varied whilst those of C-D remain fixed. The basin axes form an arcuate link between the two fold systems. Right and reverse sigmoids have formed respectively at X and Z domes on either side of the neutral dome Y.

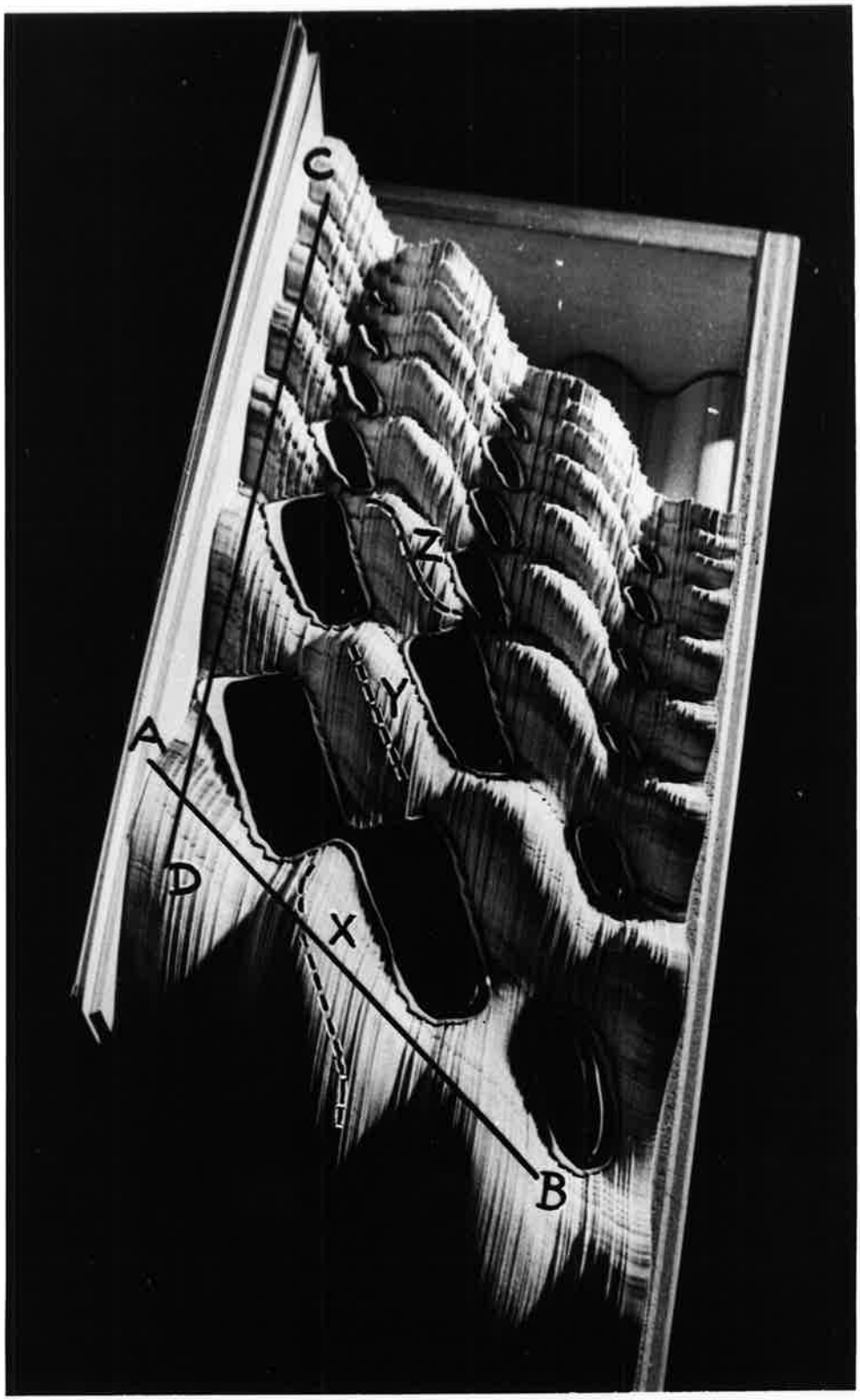

Fig. 9

FIGURE 10

A composite plan of the basin patterns in Fig. 6 and Fig. 7, showing the co-existence of right-hand echelon alignments parallel to A-B, and left-hand echelon alignments, parallel to C-D.

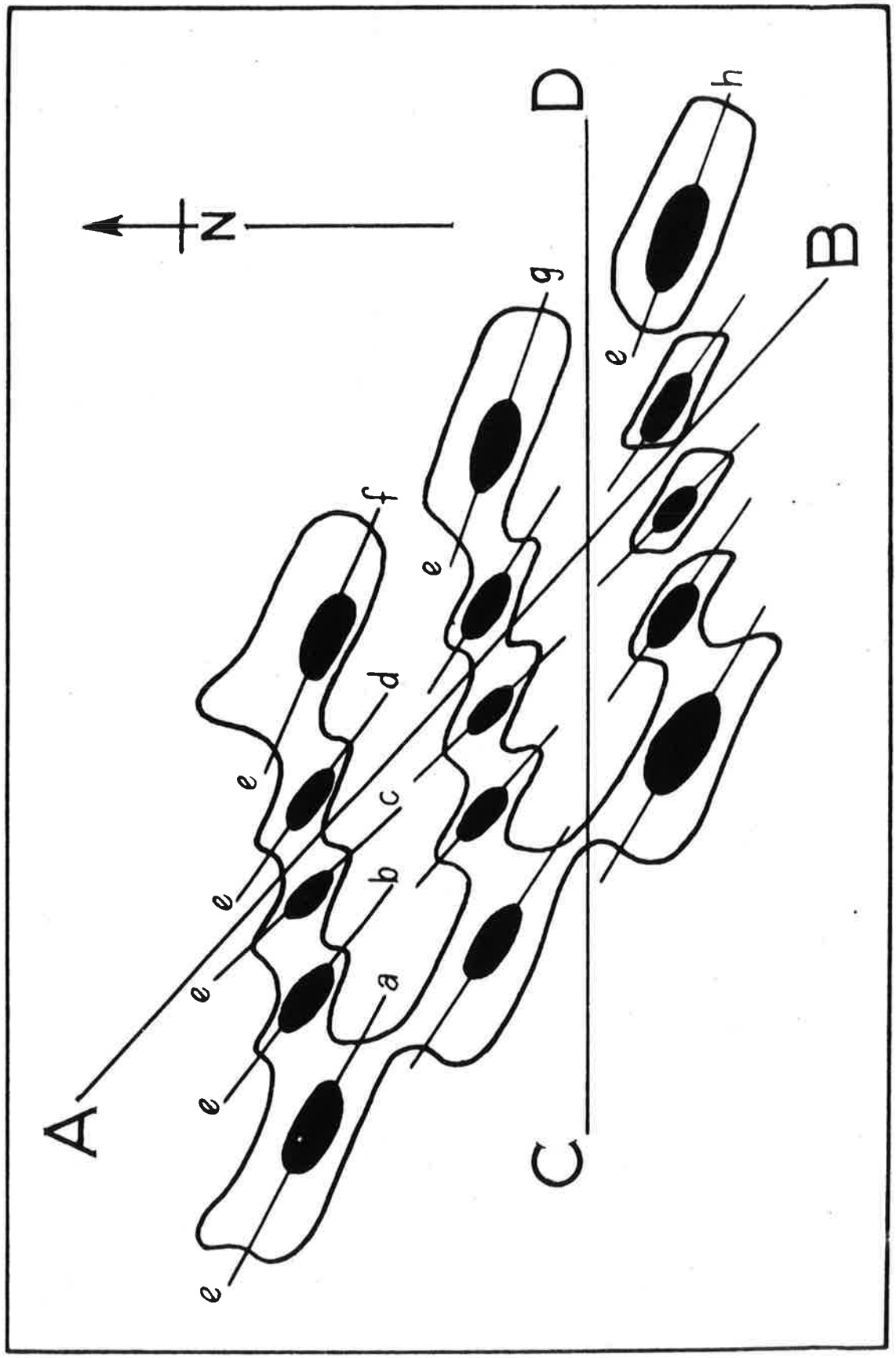
N
A
B
C
D
a
b
c
d
e
e
e
e
e
e
f
g
h

FIGURE 11

Contour relief plan of interference surface of unequal orthogonal folds, showing domes (H), basins (L), and cols (C) in their essential axial and quadrantal symmetry.

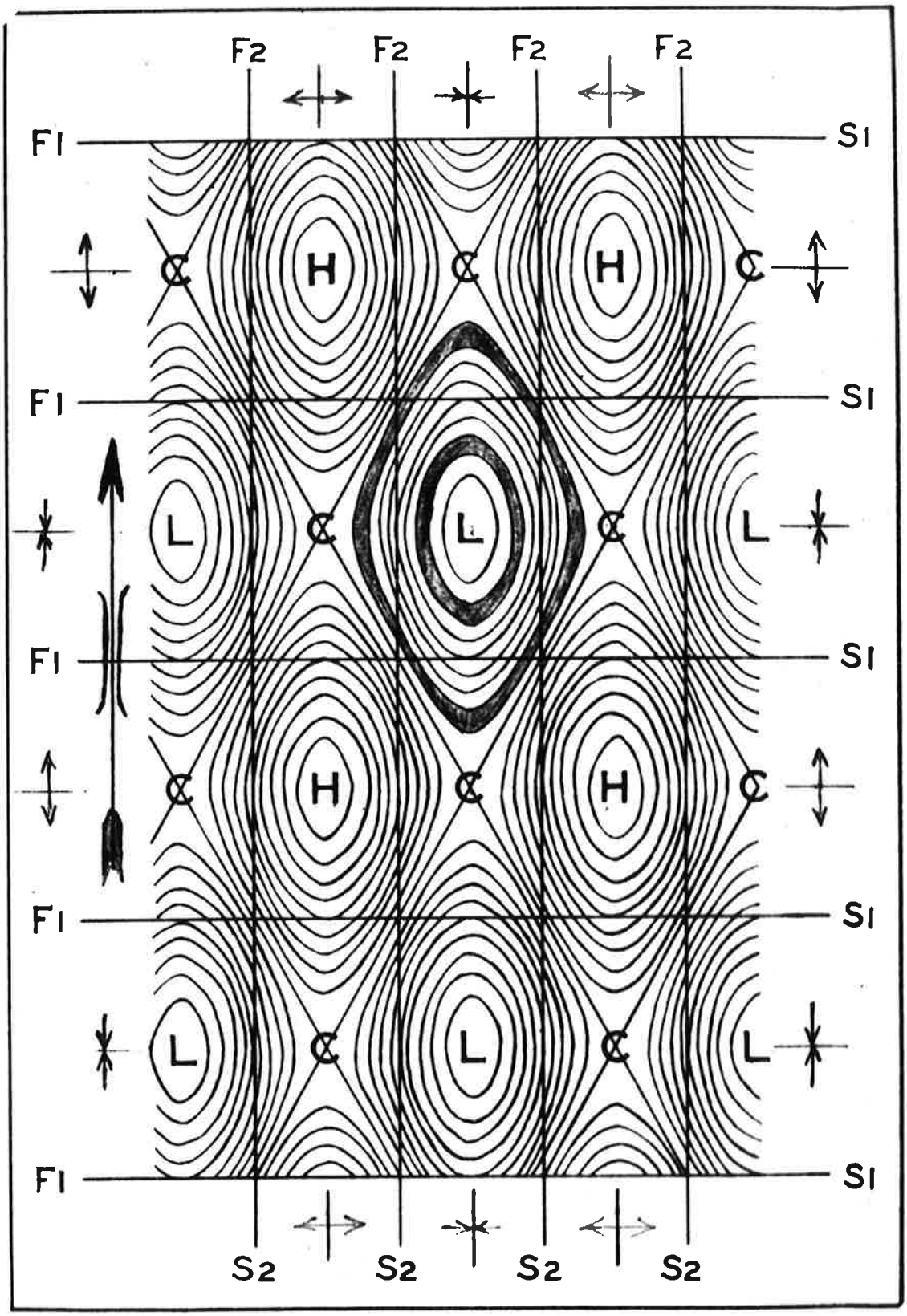

Fig. 11

FIGURE I2

In (i), two profiles are shown prior to their mutual interference. In (ii), the lower profile has been imposed on the upper by laminar transmission causing differential axial migration in the resultant interference profile.

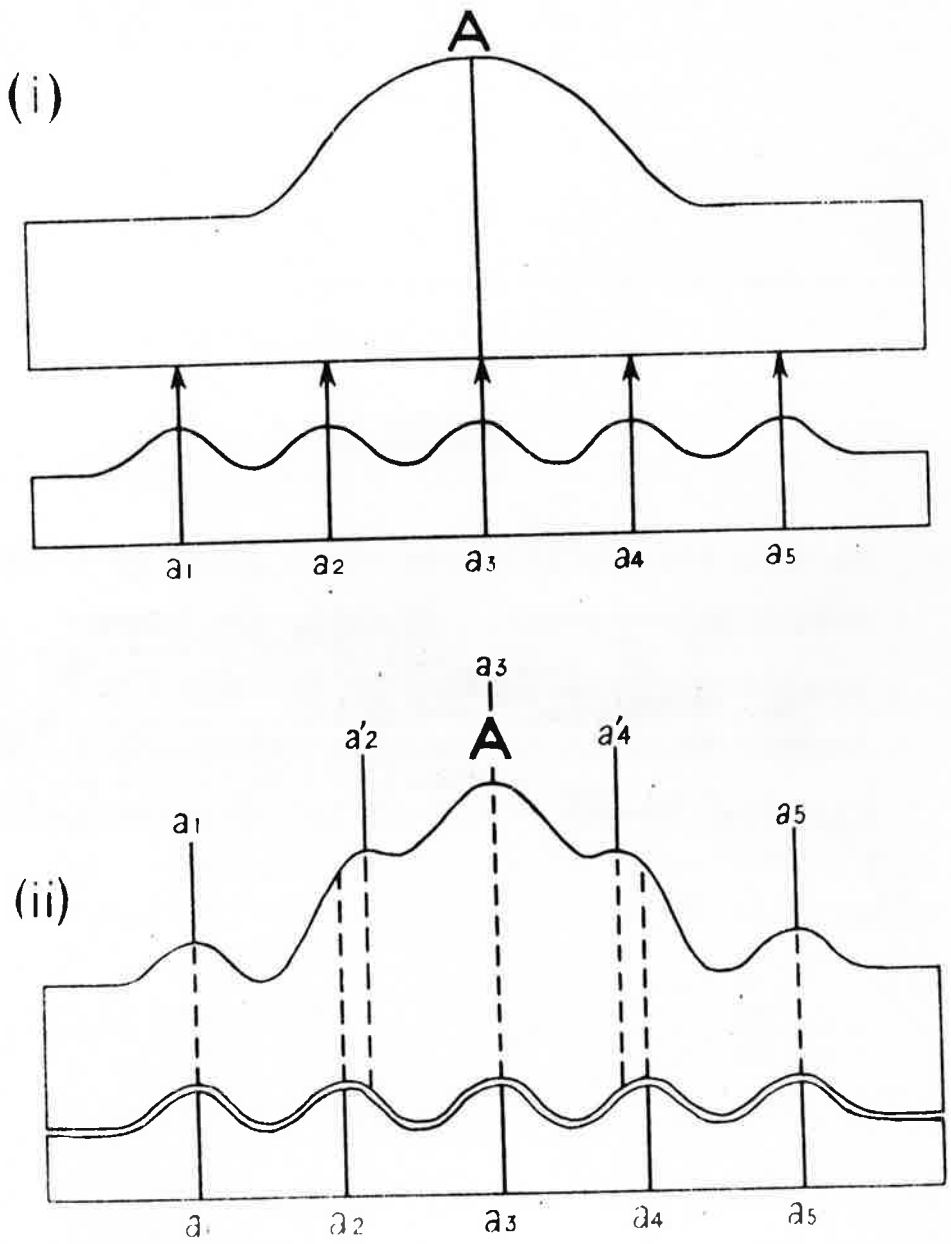

Fig. 12

FIGURE 13

Relief plan of interference dome showing right sigmoid flexure resulting from vertical interference of anticline A-A of amplitude 10 units, with an anticline B-B of equal wavelength but of amplitude 5 units. No horizontal movement is involved.

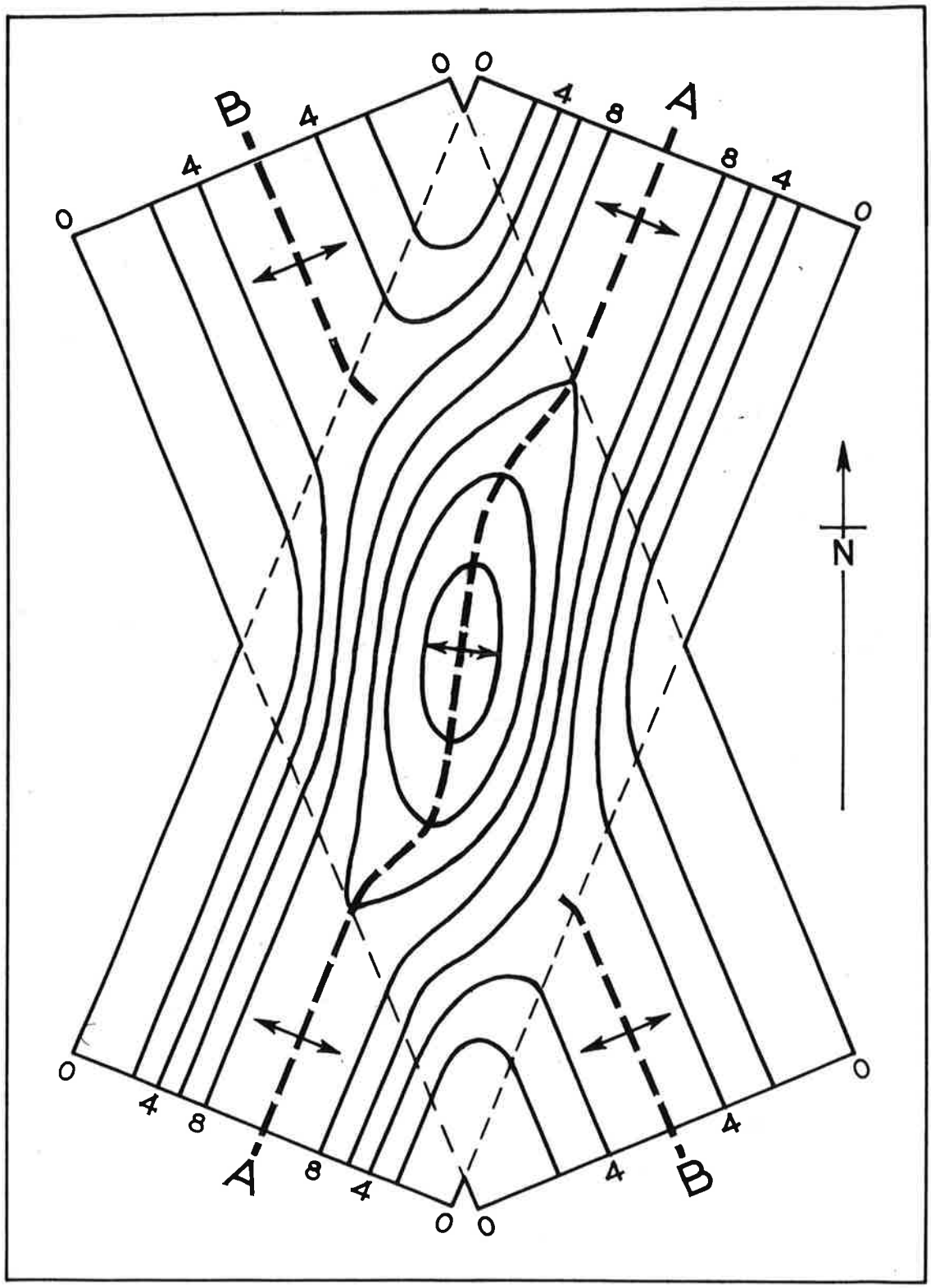

Fig. 13

FIGURE 14

The anticline B-B of Fig. 13 is here replaced by anticline C-C which has equal wavelength; but amplitude 20 units. The resultant reverse sigmoid is opposite to that of Fig. 13. There is no horizontal movement involved.

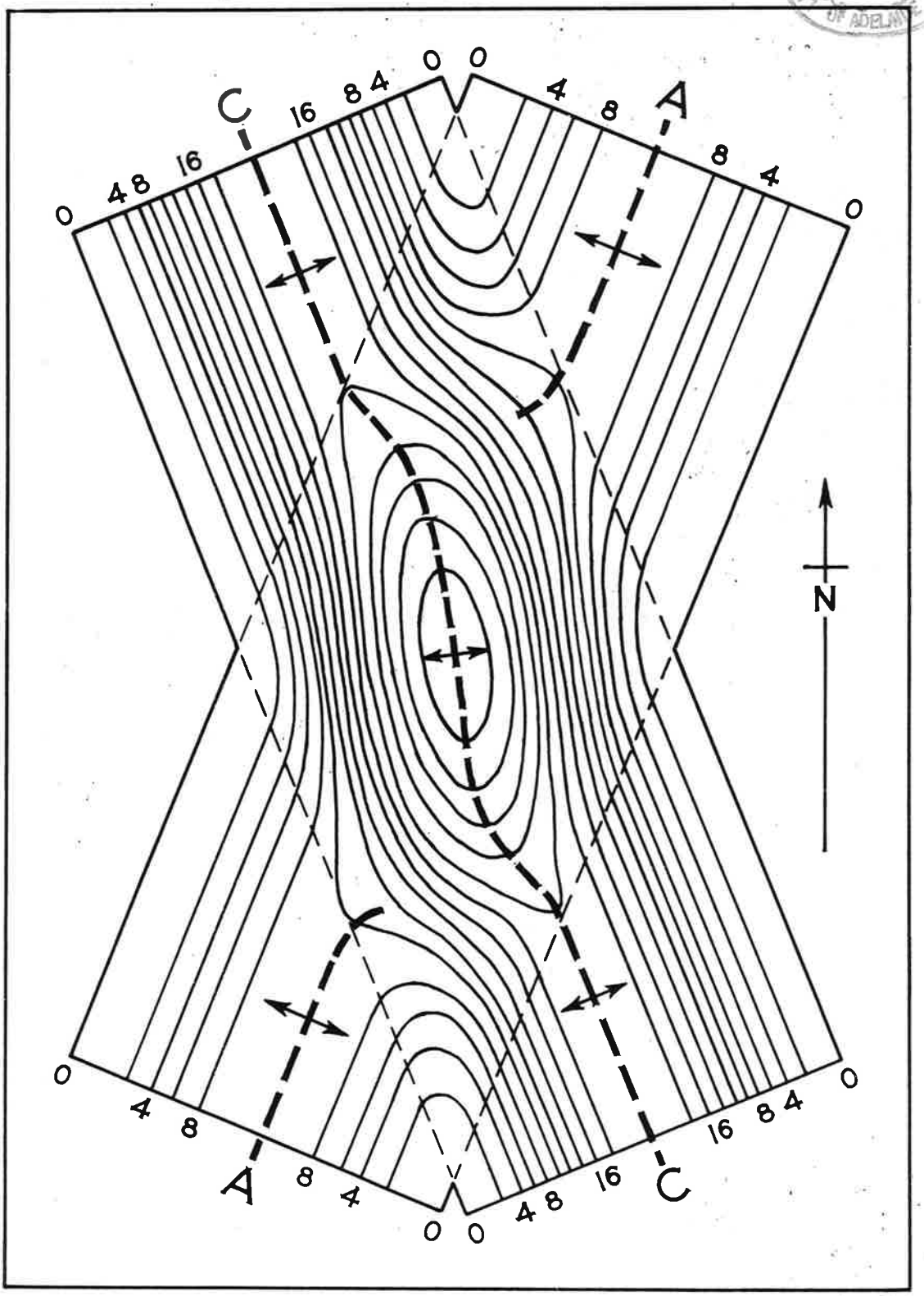

Fig. 14

FIGURE 15

Pseudo-rotational relief shapes with opposing horizontal senses and trends produced synchronously from vertical movements in a biaxial crossfold system.

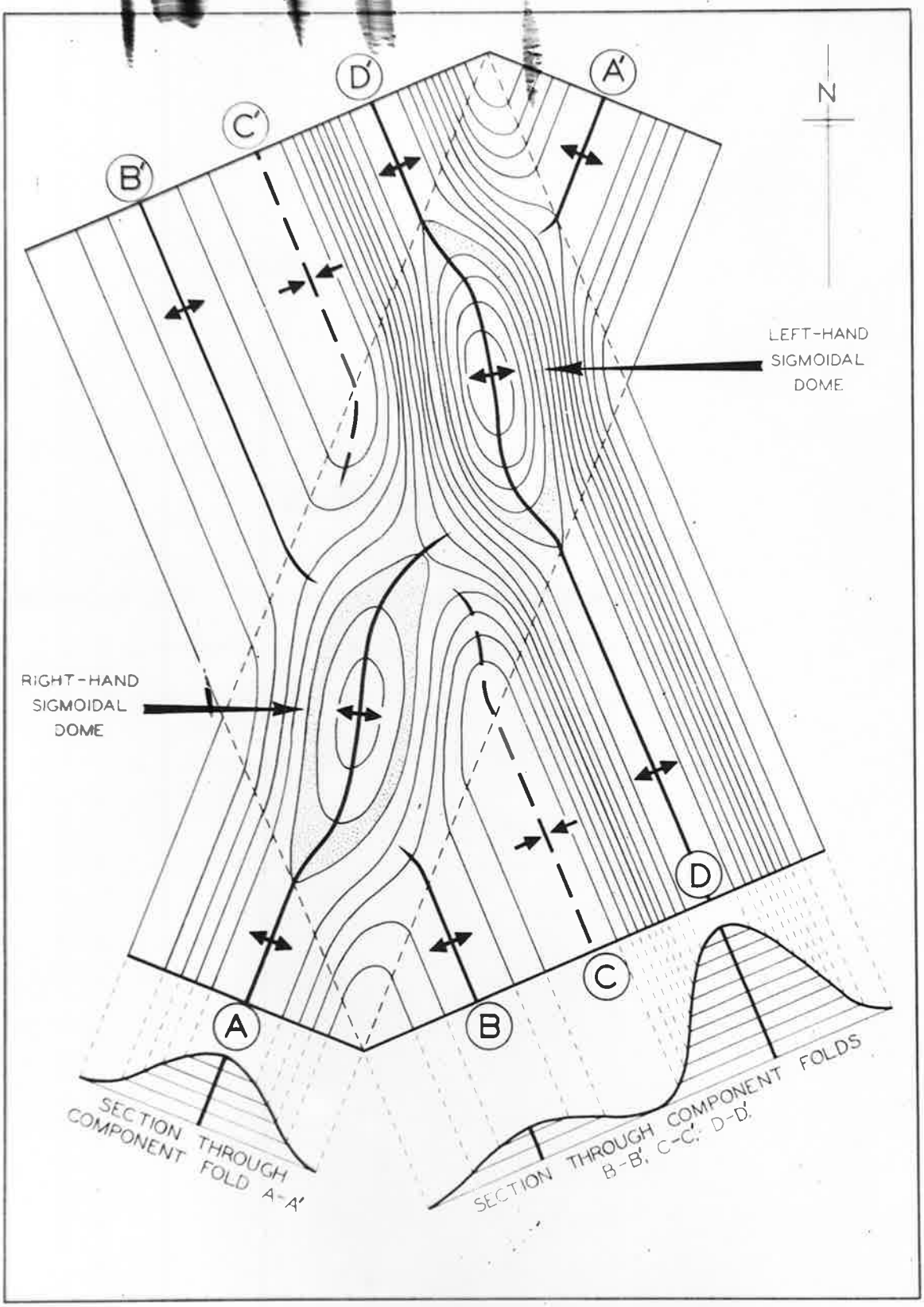
D'
A'
C'
B'
N
LEFT-HAND
SIGMOIDAL
DOME
RIGHT-HAND
SIGMOIDAL
DOME
D
C
A
B
SECTION THROUGH
COMPONENT FOLD A-A'
SECTION THROUGH COMPONENT FOLDS
B-B', C-C', D-D'

Fig. 15

FIGURE 16

Relief plan of non-orthogonal, non-equidimensional interference pattern showing interplay of opposite sigmoids and both right-hand and left-hand en echelon alignments. The axes of domes and basins are divergent. No horizontal movement is involved.

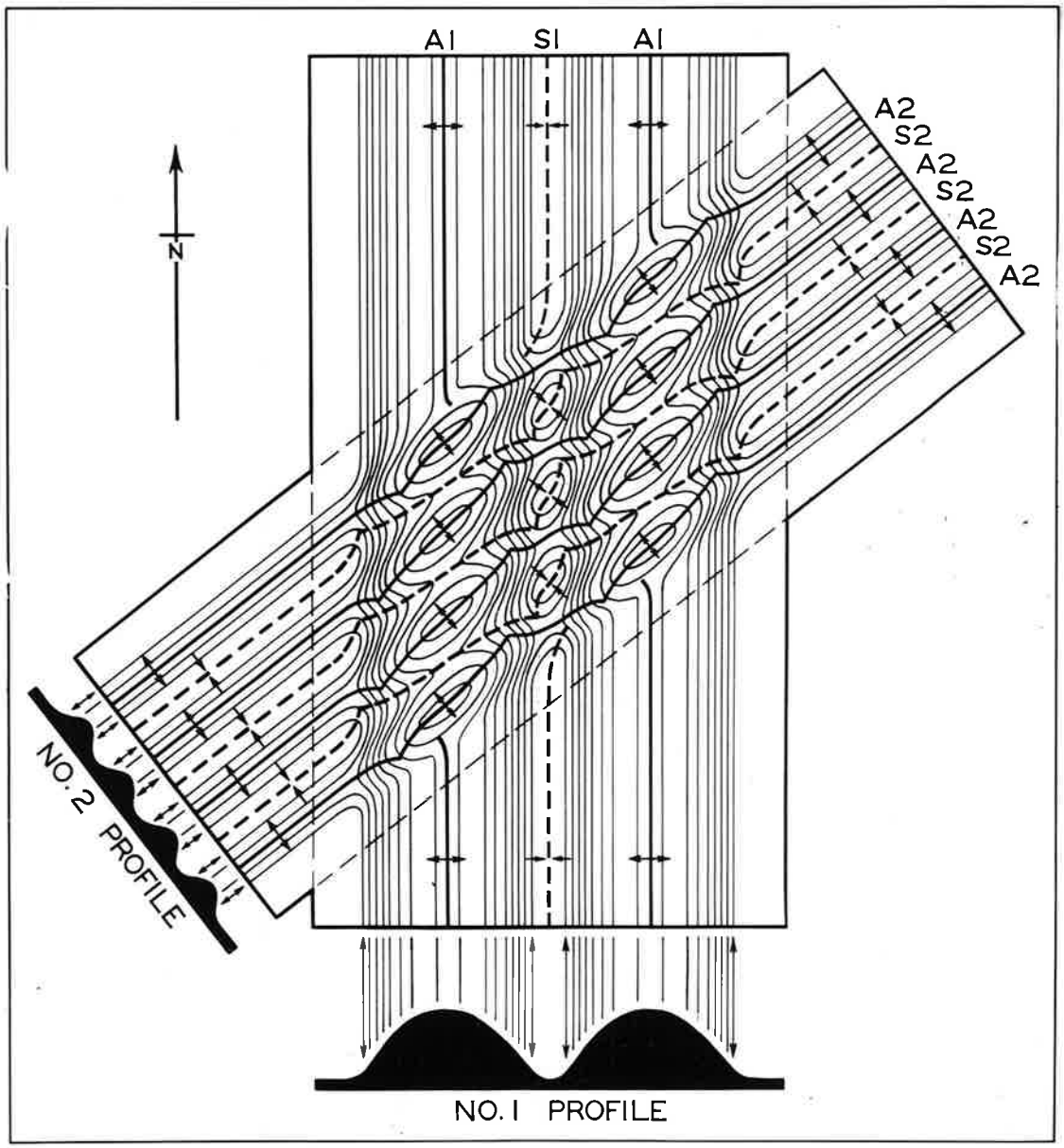

Fig. 16

FIGURE 17

The same surface as in Fig. 16, showing the alignment en echelon of zones of maximum shear, and the generalized structure in which the greater axial continuity is maintained by folds with the greater crestal curvature (A2-S2 system.)

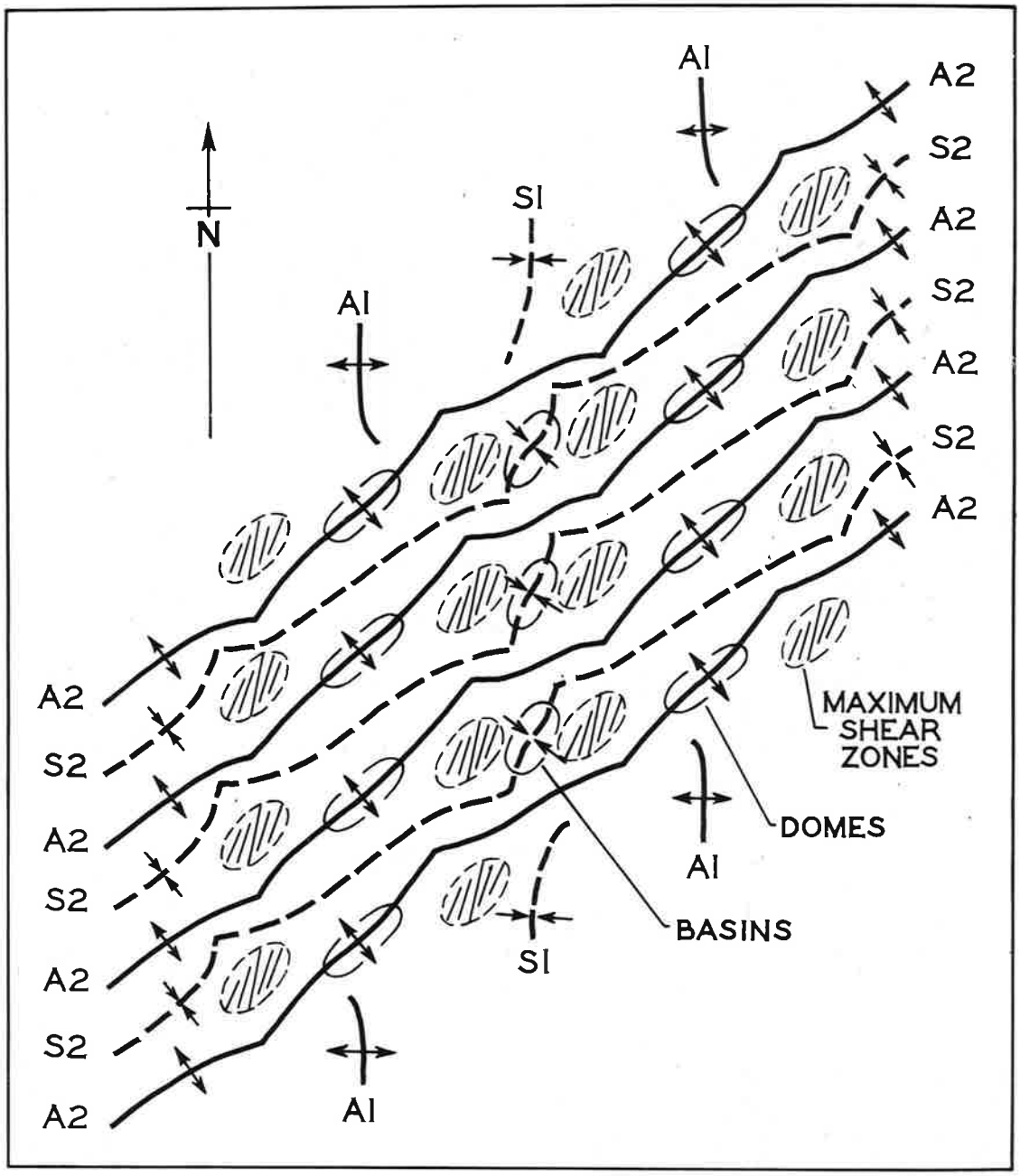

Fig. 17

FIGURE 18

Specimen of cards printed with continuous succession of similar profiles to provide internal repetition of interference surfaces within the card pack. (Symbols added for text explanation).

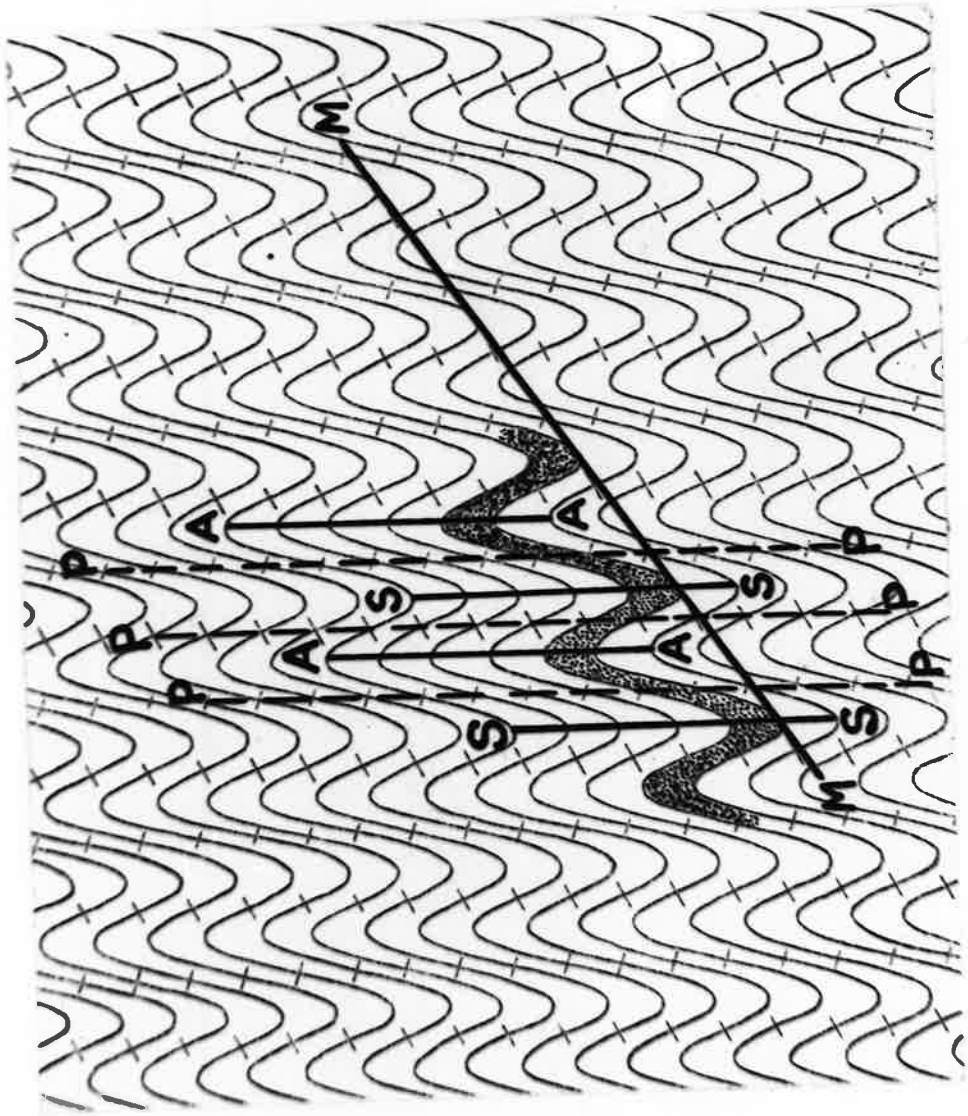

Fig. 18

FIGURE 19

Printed card model showing interference surface intact in foreground, and truncated in background to expose traces of successive surfaces.

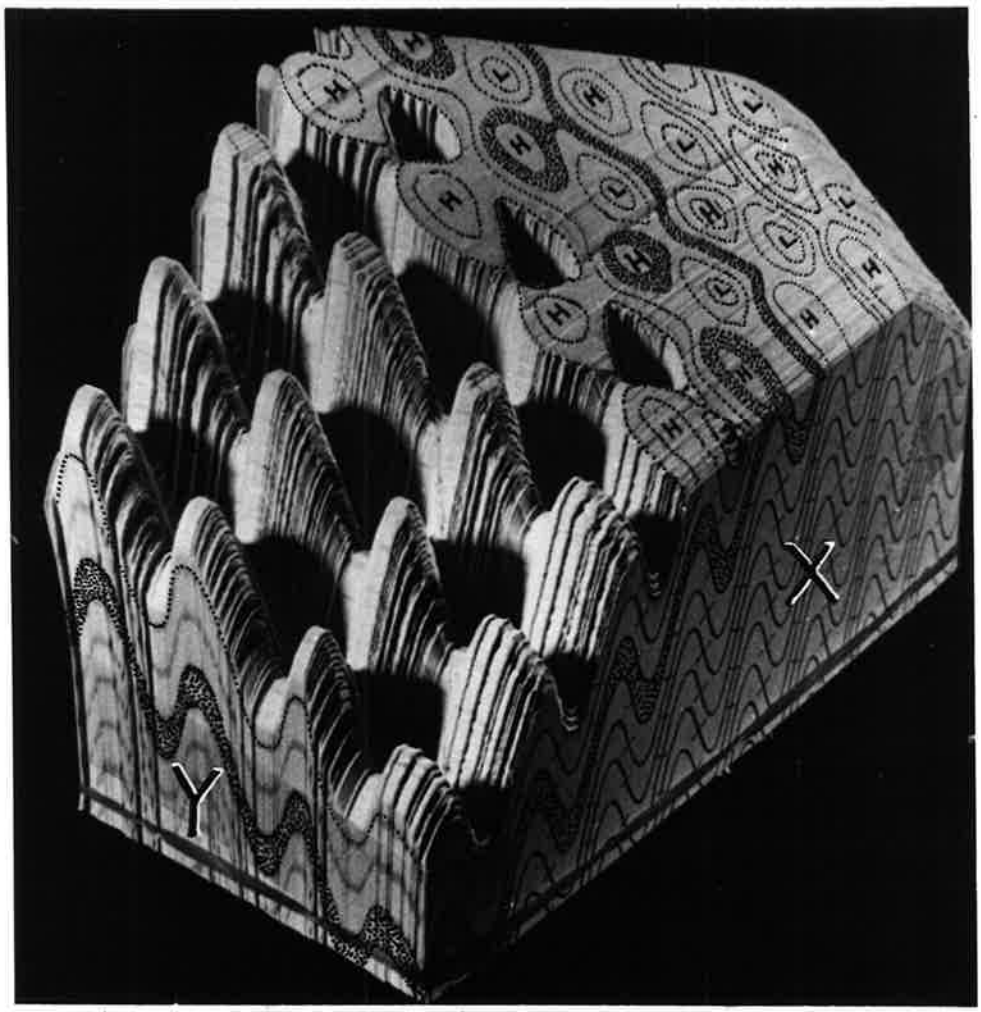

Fig. 19

FIGURE 20

PIane cut through printed card model exposing succession of interference surfaces forming truncated domes (H) and basins (L). One stratum is accentuated to show predominance of quadrantal strike.

FIGURE 21

A plane similar to Fig. 20, but with an axial strike predominating. The essential difference between Fig. 20 and Fig. 21 is in the strike of the surface of the "mega-slope" on which the smaller structures are set.

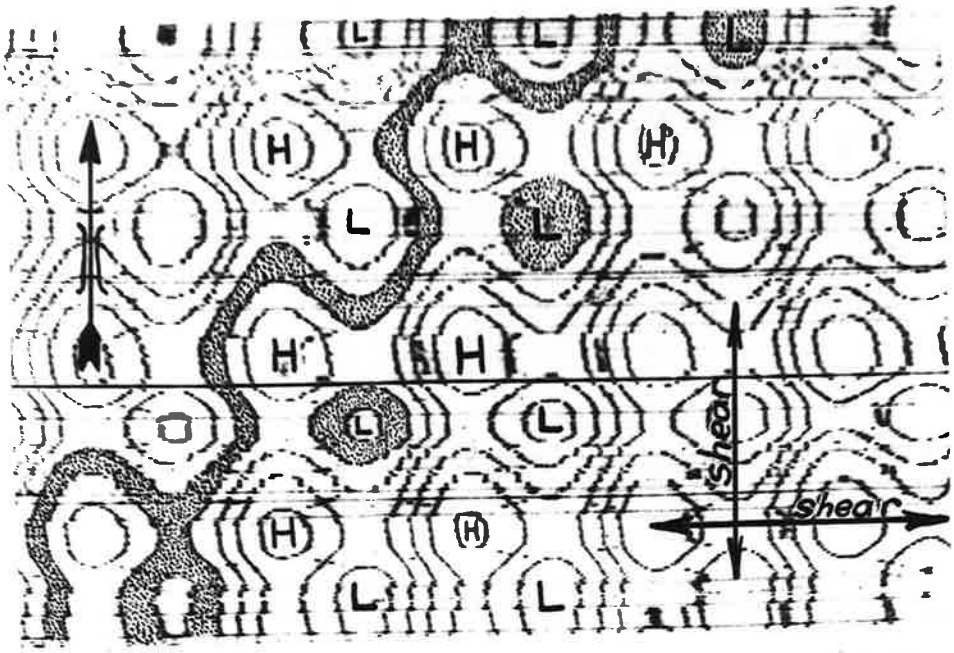

Fig. 20

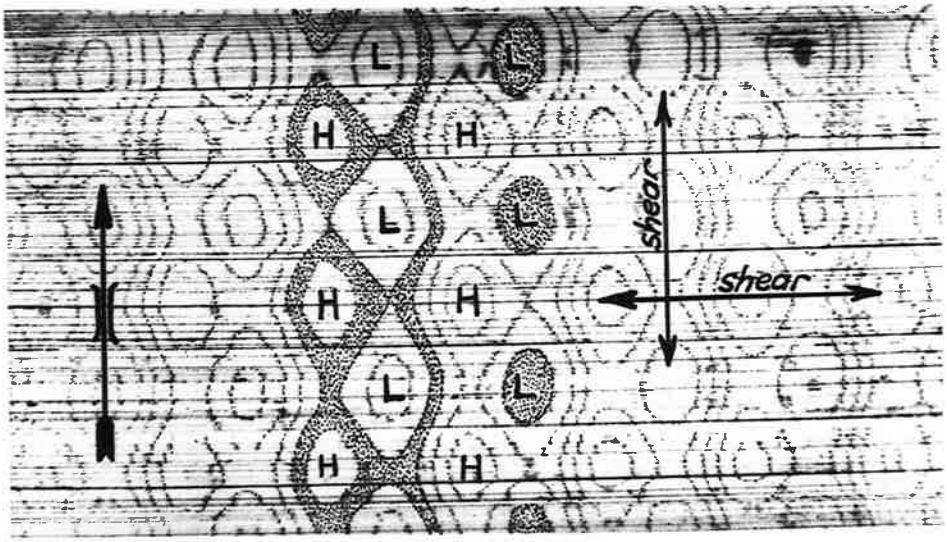

Fig. 21

FIGURE 22

A curved surface cut on a printed card model to show the resulting variation in the interference traces.

Fig. 22

FIGURE 23

A vertical section of discordant surfaces prior to receiving the differential profile of the template, T, by vertical differential movement along the fold axes A1, S and A2.

FIGURE 24

The profile of T imposed on the section in Fig. 23 results in the dislocation and deflection of axes in successive strata. Two closures in stratum Y are marked.

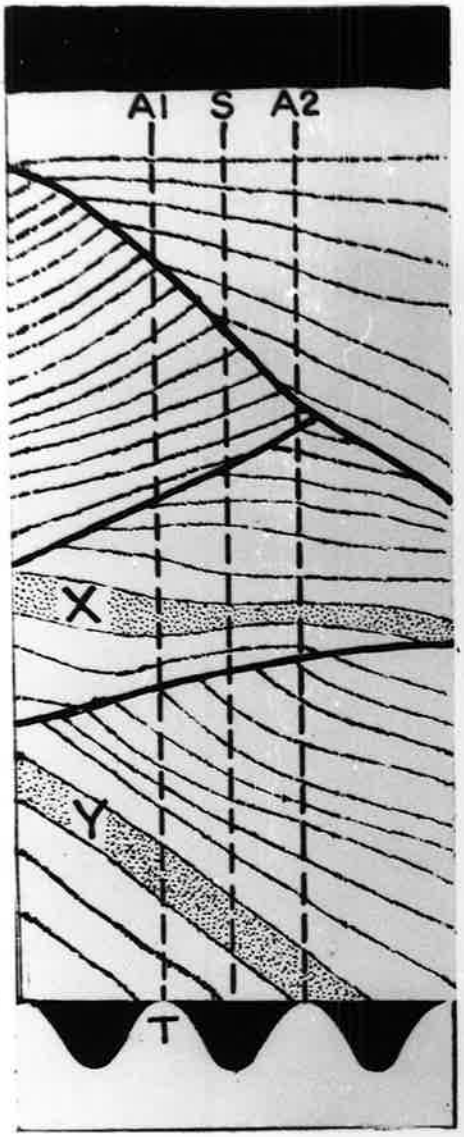

Fig. 23

Fig. 24

FIGURE 25

The result of superposing a vertical clockwise "regional shear" on the section in Fig. 24 is to produce a change in axial spacing and degree of closure of structures in stratum Y.

FIGURE 26

The result of superposing an anticlockwise "regional shear" on the section in Fig. 25 is to cause reciprocal movements of axial spacing.

Fig. 25

Fig. 26

FIGURE 27

The shape of a horizontal fold interference surface, (AaBbC), transmitted vertically to an inclined surface, (DdEeF), results in the lateral migration of corresponding domal crests.

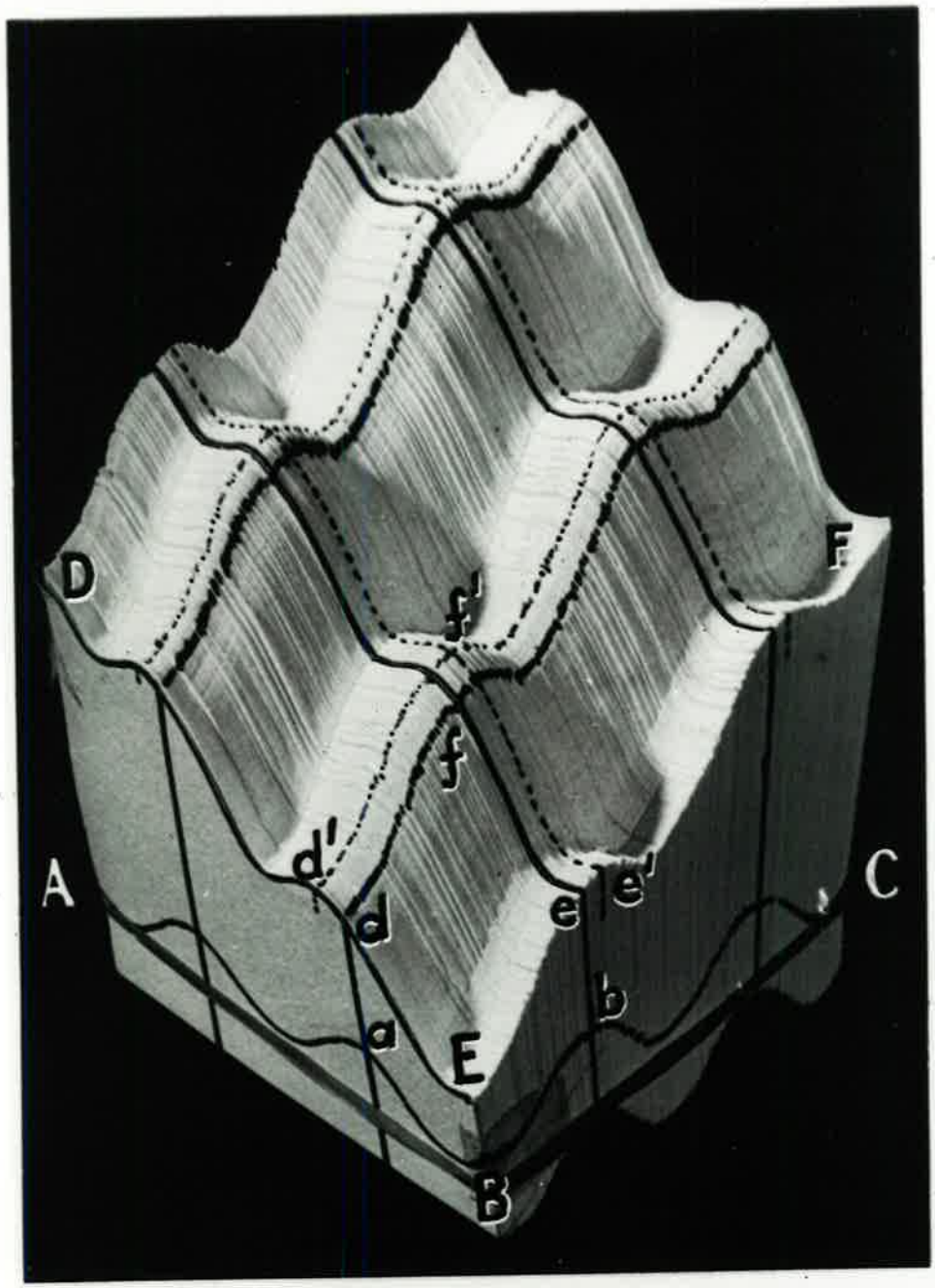

Fig. 27.